

Virus Removal by Biogenic Cerium

BART DE GUSSEME,[†] GIJS DU LAING,[‡]
TOM HENNEBEL,[†] PIET RENARD,[†]
DEV CHIDAMBARAM,[§] JEFFREY P. FITTS,^{||}
ELS BRUNEEL,[‡] ISABEL VAN DRIESSE,[‡]
KIM VERBEKEN,[#] NICO BOON,[†] AND
WILLY VERSTRAETE^{*,†}

Laboratory of Microbial Ecology and Technology (LabMET), Ghent University, Coupure Links 653, B-9000 Gent, Belgium, Laboratory of Analytical Chemistry and Applied Ecochemistry (Ecochem), Ghent University, Coupure Links 653, B-9000 Gent, Belgium, Chemical and Materials Engineering, University of Nevada Reno, Chemical and Metallurgical Engineering Department, 1664 N. Virginia St. - MS 388, Reno, Nevada 89557, Environmental Sciences Department, Brookhaven National Laboratory, Building 830, Upton, New York 11973, Department of Inorganic and Physical Chemistry, Ghent University, Krijgslaan 281-283, B-9000 Gent, Belgium, and Department of Metallurgy and Materials Science, Ghent University, Technology Park 903, B-9052 Gent, Belgium

Received January 12, 2010. Revised manuscript received June 9, 2010. Accepted June 30, 2010.

The rare earth element cerium has been known to exert antifungal and antibacterial properties in the oxidation states +III and +IV. This study reports on an innovative strategy for virus removal in drinking water by the combination of Ce(III) on a bacterial carrier matrix. The biogenic cerium (bio-Ce) was produced by addition of aqueous Ce(III) to actively growing cultures of either freshwater manganese-oxidizing bacteria (MOB) *Leptothrix discophora* or *Pseudomonas putida* MnB29. X-ray absorption spectroscopy results indicated that Ce remained in its trivalent state on the bacterial surface. The spectra were consistent with Ce(III) ions associated with the phosphoryl groups of the bacterial cell wall. In disinfection assays using a bacteriophage as model, it was demonstrated that bio-Ce exhibited antiviral properties. A 4.4 log decrease of the phage was observed after 2 h of contact with 50 mg L⁻¹ bio-Ce. Given the fact that virus removal with 50 mg L⁻¹ Ce(III) as CeNO₃ was lower, the presence of the bacterial carrier matrix in bio-Ce significantly enhanced virus removal.

Introduction

Cerium (⁵⁸Ce) is the second lightest member of the lanthanides or rare earth elements (REE). In physiological

solutions, most of these REE are only stable in the trivalent oxidation state (+III), with Eu(II) and Ce(IV) being the only exceptions (1). Both Ce(III) and Ce(IV) containing compounds were reported to exert antifungal, bacteriostatic, and bactericidal activity (2, 3). Ce(III) in the form of Ce(NO₃)₃ was shown to be an effective bacteriostatic agent against a wide variety of species. Sobek and Talburt studied the effect of cerium nitrate on *E. coli* and have demonstrated inhibition of the cellular respiration, oxygen uptake, and glucose metabolism (3). Nonspecific binding to proteins or binding to and inactivation of phosphate compounds were suggested to be the main mechanism. In addition, Ce(III) is also known to replace Ca(II) in many biomolecules, without necessarily substituting for it functionally (4). In 1976, Monafó et al. (5) suggested a synergistic interaction between cerium nitrate and silver sulphadiazine. This combination is used in two commercially available products for the treatment of burn wounds: Flamacerium and Dermacerium (6). Ce(IV), in the form of CeO₂ nanoparticles, exhibits bactericidal and virucidal activities. Thill et al. (7) demonstrated that a large amount of CeO₂ can be adsorbed on the outer membrane of *Escherichia coli* and that Ce(IV) was reduced to Ce(III) by the bacterial cell wall membrane. Both phenomena were related to the cytotoxicity to the cells. The capacity of CeO₂ nanoparticles for virus removal was shown by Link et al. (8). The nanoparticles possess a high binding capacity for nucleic acids and could remove viruses including HIV-1 from aqueous solutions.

Cell-associated metals and metal oxides are currently of interest for advanced water treatment and disinfection of (drinking) water in particular. For example, the microbiological production of manganese oxides and nanoparticles of silver or palladium, has opened up a window of new applications (9). The association of these metals and metal oxides with a microscale bacterial carrier matrix allows their retention in reactor systems by means of microfiltration (10). Moreover, the bacterial carrier acts as a stabilizing agent, thus reducing leaching of the metal species into the environment. In this way, biogenic metals can be applied as catalysts in the degradation of pollutants, or for disinfection of drinking water.

In natural environments, microorganisms play an important role in the geochemistry of REE and other elements (11, 12). For example, the oxidation of Mn(II) to Mn(III,IV) oxides by manganese-oxidizing bacteria (MOB) is considered to be a more important pathway in aqueous environments than chemical oxidation (13, 14). Moffett (15, 16) has examined the interaction between MOB and Ce in the marine environment and suggested that Ce(III) and Mn(II) are oxidized by the same bacterial pathway in seawater. Based on his results, it was hypothesized that Ce(III) oxidation decreased with increasing Mn(II) concentration, indicating inhibition, possibly through competition. On the contrary, Ohnuki et al. (17) showed that freshwater MOB oxidize Mn(II) to Mn(III,IV) but do not oxidize Ce(III). By means of XANES analysis, it was demonstrated that the biologically formed Mn(III,IV) precipitations accumulated Ce(III) and then abiotically oxidized it to Ce(IV).

The aim of this study was to associate cerium with a bacterial carrier matrix to disinfect water contaminated with bacteriophage UZ1. This phage, which infects *Enterobacter aerogenes*, serves as model for enteric viruses (18). Aqueous Ce(III) was added to cultures of the freshwater MOB *Leptothrix discophora* and *Pseudomonas putida* MnB29 (19), in the absence of Mn(II). Electron microscopy, X-ray diffraction and X-ray spectroscopy results suggest that the

* Corresponding author phone: +32 9 264 59 76; fax: +32 9 264 62 48; e-mail: Willy.Verstraete@UGent.be.

[†] Laboratory of Microbial Ecology and Technology (LabMET), Ghent University.

[‡] Laboratory of Analytical Chemistry and Applied Ecochemistry (Ecochem), Ghent University.

[§] Chemical and Metallurgical Engineering Department, University of Nevada Reno.

^{||} Environmental Sciences Department, Brookhaven National Laboratory.

[‡] Department of Inorganic and Physical Chemistry, Ghent University.

[#] Department of Metallurgy and Materials Science, Ghent University.

interaction between Ce(III) and phosphoryl groups at the bacterial surface is responsible for the observed antiviral activity.

Experimental Section

Removal of Soluble Ce by MOB. Overnight cultures of the MOB *L. discophora* and *P. putida* MnB29 (LMG 8142 and LMG 2323, BCCM/LMG collection, Ghent University, Belgium) were cultivated in a medium described by Boogerd and de Vrind (20) at 28 °C on a platform shaker (120 rpm). Subsequently, 1 mL of the cultures was inoculated into sterile 250 mL Erlenmeyer flasks, supplemented with 150 mL of sterile growth medium to which 140 mg Ce(III) L⁻¹ was added as CeCl₃ (Sigma-Aldrich, St. Louis, MO). During incubation, bacterial growth was followed by means of the optical density at 610 nm (OD_{610 nm}) and the volatile suspended solids (VSS) concentration (21). As a control experiment, a similar batch incubation experiment was set up with *L. discophora*, in which 1 g sodium azide L⁻¹ (Sigma-Aldrich) was added to the growth medium 48 h after incubation, to inhibit bacterial growth (22). A biomass-free control experiment in the same growth medium was included as well. All incubation experiments were performed in triplicate at 28 °C on a platform shaker (120 rpm) for 14 days. Samples were taken at regular intervals, filtered over a 0.22 µm filter (Millipore, Billerica, MA) and kept at 4 °C for further analysis. To determine the soluble cerium concentration, inductively coupled plasma optical emission spectrometry (ICP-OES) was used (Vista MPX, Varian, Palo Alto, CA). The limit of detection (LOD) of ICP-OES was 0.2 mg L⁻¹.

Characterization. Samples of *P. putida* MnB29 biomass (grown with and without cerium) were taken after 14 days of incubation. The cells were centrifuged (8500g, 10 min) and washed three times with deionized water. The term “biogenic” cerium or “bio-Ce” refers to the biological generation of a ligand (i.e., the *P. putida* biomass) that anchors soluble or colloidal Ce and keeps it cell-associated.

For SEM analyses, the samples of *P. putida* MnB29 biomass grown without cerium were fixed according to Mast et al. (23) but a KH₂PO₄/K₂HPO₄ buffer (P-buffer) (2.56 and 14.14 g L⁻¹, respectively) was used to keep the bacterial cells intact. The samples of bio-Ce were examined on a double-sided carbon tape (amorphous structure with good conductivity) under a FEI SEM XL30 (Eindhoven, The Netherlands) equipped with a LaB₆ filament and an EDX detector (EDAX, Tilburg, The Netherlands). By means of EDX, the elemental composition of the sample surface can be determined by comparing the peaks with standards for the elements of interest, according to the Cliff-Lorimer method (24). Before putting the samples in the SEM, a thin gold layer was applied with a Baltic SCD005 Sputter Coater at a pressure of 0.1 mbar for 60s with a current of 40 mA.

XRD measurements were performed with a Siemens D5000 diffractometer (Munich, Germany) with Bragg-Brentano optics and filtered Cu-K_α radiation (40 kV and 50 mA). With XRD, crystallinity and the oxidation of cerium in the crystal can be analyzed. Samples were dried at room temperature.

By means of XANES, the predominant oxidation state and the nature of the bonding between Ce and the MOB were examined. XANES spectra were collected at beamline X11 of the National Synchrotron Light Source (NSLS) at the Brookhaven National Laboratory (New York, NY). The beamline was equipped with a S(111) monochromator and a Lytle fluorescence detector. All spectra were collected at room temperature and 50% detuning of the monochromator in order to minimize higher order harmonics. X-ray absorption coefficients were measured from 150 eV below to 400 eV above the Ce L_{III}-edge. Absolute X-ray energy calibration was based on the first inflection point of a Cr metal foil (5989.0

eV), which was collected in transmission mode either as an internal calibration during each scan or before and after a set of scans. Powder samples of CeCl₃, Ce(NO₃)₃, Ce₂(CO₃)₃·2H₂O and CePO₄·H₂O were used as Ce(III) standards. Ce(SO₄)₂, Ce(OH)₄, and CeO₂ were used as Ce(IV) standards. All model compound samples were ground and mixed with boron nitride to optimize absorbance for transmission mode data collection. The bio-Ce samples were centrifuged and the fully hydrated pellets were sealed in an ultrathin X-ray grade polypropylene sample bag. XANES spectra normalization, calibration, averaging, fingerprinting, and peak-fitting were performed using Athena software (25).

Detection of Bacteriophage UZ1. A stock of bacteriophage UZ1 was prepared as previously described (26). To detect phages, the soft agar layer method described by Adams (27) was applied, using serial 10-fold dilutions of the samples. As a host, a midlog phase *E. aerogenes* BE1 culture (LMG 22092, BCCM/LMG) was used. Phages were counted as plaque forming units (pfu) and the phage concentration was expressed as pfu mL⁻¹. In the plaque assays, the LOD was determined to be 1.0 × 10² pfu mL⁻¹. When no viruses were detected in the samples, the LOD was used as a conservative estimate for the UZ1 concentration.

Disinfection Assay on Bacteriophage UZ1. All disinfection assays were performed with bottled natural source water (Spa Blauw, Spadel, Brussels, Belgium). The listed concentrations of biogenic cerium (in mg bio-Ce L⁻¹) refer to the pure Ce concentrations associated with the bacterial biomass (weight of the biomass not included). Disinfection assays were conducted in triplicate in sterilized 250 mL Erlenmeyer flasks placed on a shaker (120 rpm) at 28 °C for 2 h. Samples of bio-Ce were harvested after 14 days of incubation by centrifugation (8500g, 10 min), washed twice with deionized water and added to 100 mL of bottled source water to final concentrations of 0, 5, 50, 100, 250, and 500 mg bio-Ce L⁻¹ (pH 5.5). Subsequently, 50 mg bio-Ce L⁻¹ was added to bottled source water in a 24 h experiment. This suspension was supplemented with 100 µL of a phage stock solution (2.6 ± 2.3 × 10⁹ pfu mL⁻¹). Controls were water (biomass-free control), and water supplemented with *P. putida* MnB29 cultures similarly grown in Ce-free medium and washed twice with water (same OD_{610 nm} as biomass with Ce) (pH 5.5). Samples were taken at regular intervals, filtered over a 0.22 µm filter (Millipore, Billerica, MA) to remove the biomass and associated cerium, then stored at 4 °C for further analysis. Inactivation was expressed as log decrease (with the % decrease between parentheses).

Three comparative disinfection assays were carried out in water supplemented with Ce(NO₃)₃ (Sigma-Aldrich), CePO₄·H₂O (Sigma-Aldrich) (both in a final concentration of 50 mg Ce(III) L⁻¹) and CeO₂ nanoparticles (Umicore Research, Olen, Belgium) with an average particle size of 25 ± 15 nm (final concentration of 50 mg Ce(IV) L⁻¹). For each experiment, three replicates were incubated for 24 h and samples were taken at regular intervals and immediately analyzed by plaque assays.

Statistical Analyses. SPSS for Windows version 15.0 was used for statistical analysis. Tests for normality of data and homogeneity of the variances were performed using the Kolmogorov–Smirnov and Levene’s test, respectively. One-way analysis of variance was used to compare the mean values of the normal distributed data. *P*-values ≤ 0.05 were considered significant.

Results

Batch Incubation Experiments. Figure 1 shows the results of the incubation experiments. No removal of soluble Ce was detected in the biomass-free growth medium (C₀ = 140 ± 6 mg Ce(III) L⁻¹). In contrast, when MOB were incubated in the growth medium with the same Ce(III) concentration,

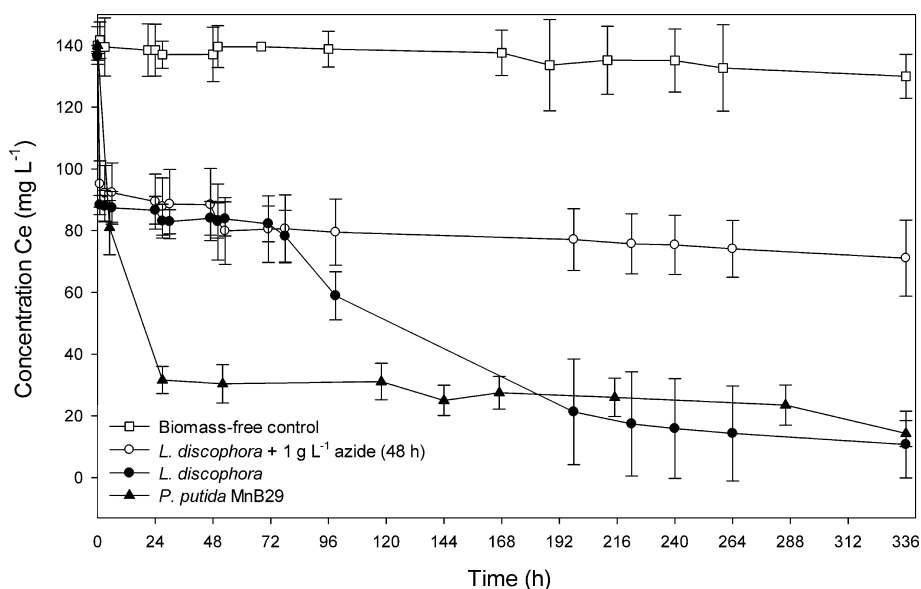


FIGURE 1. Soluble Ce concentration as a function of time during 14 day incubations of MOB *L. discophora* and *P. putida* MnB29, in growth medium supplemented with 140 mg Ce(III) L⁻¹. To inhibit bacterial growth in a control experiment, 1 g azide L⁻¹ was added to a *L. discophora* culture, 48 h after inoculation. Results from a biomass-free control in the growth medium are also shown.

a significant decline was observed compared to the biomass-free control ($p < 0.001$ for both species). In the case of *P. putida* MnB29, soluble Ce decreased by 59.0 ± 8.8 mg soluble Ce L⁻¹ after 1 h (42.2% removal). After 24 h of incubation, the soluble Ce concentration decreased to 31.6 ± 4.4 mg L⁻¹ (77% removal). The subsequent, slower removal was similar to that observed in the biomass-free control, indicating that cell-associated Ce removal was complete after 24 h for *P. putida* MnB29. A concentration of 14.3 ± 4.2 mg soluble Ce L⁻¹ was obtained after 14 days (=90% removal). During incubation, bacterial growth was confirmed by an increase in the VSS concentration from 126 ± 9 mg L⁻¹ to 290 ± 28 mg L⁻¹ after 14 days, and an increase in the OD_{610 nm} from 0.213 ± 0.034 at the start to 1.310 ± 0.076 in the stationary phase, which was reached after 48 h (relative to the biomass-free growth medium).

Incubation of *L. discophora* resulted in a removal of 48.3 ± 3.1 mg soluble Ce L⁻¹ within one hour (35% removal). Subsequently, a lag in removal was observed until 78 h after incubation when the soluble Ce concentration started to decrease and a final concentration of 8.1 ± 6.5 mg soluble Ce L⁻¹ was reached after 14 days (=92% removal). In the control experiment, similar removal was observed in the first hour, before the addition of 1 g azide L⁻¹ (41.2 ± 7.5 mg soluble Ce L⁻¹ removed or 29.5% removal). After azide addition at 48 h, soluble Ce was removed slower and at a similar rate as the biomass-free control. A final concentration of 65.1 ± 12.1 mg soluble Ce L⁻¹ was reached after 14 days of incubation (=54% removal) in the azide-poisoned control.

Characterization of Biogenic Cerium. Secondary Electron (SE) images of the fixed *P. putida* MnB29 grown in medium without Ce(III) and fixed with P-buffer showed the rod-shaped cells with a smooth surface (Figure 2A). Samples grown in the presence of Ce(III) were not fixed to prevent precipitation of CePO₄. Therefore, the cell shape of *P. putida* MnB29 was lost as an artifact of the vacuum applied in a SEM (Figure 2B). Yet, no crystals were found on the bacterial surface. The EDX spectrum of the latter bacterial surface is shown in Figure 2C. An approximate calculation using EDAX software showed that Ce was present on the biomass at 2–3%. The resulting anchoring of soluble or colloidal cerium onto the bacterial carrier matrix will be further referred to as biogenic cerium or bio-Ce.

XRD, XPS, and XANES analyses were performed to further characterize the biogenic cerium. XRD analysis did not show any crystallinity (data not shown). The results of the XPS analysis are given as Supporting Information. The XPS cerium 3d core level spectrum of bio-Ce suggest that the oxidation state of Ce in the samples was +III (Supporting Information Figure S11). XANES spectroscopy results confirm that the fully hydrated bio-Ce samples contain Ce(III). Figure 3 compares the XANES spectra of Ce(III) and Ce(IV) containing compounds. The absorption edge energy of a XANES spectrum, which is conventionally defined as the first inflection point in the rising edge of the spectrum, is used to compare oxidation states of a given element. The adsorption edge energies of the spectra shown in Figure 3 fall into two clearly defined groups. The first group of Ce(III) compounds Ce(NO₃)₃ (5723.9 eV), CeCl₃ (5724.1 eV), Ce₂(CO₃)₃·2H₂O (5724.2 eV), and CePO₄·H₂O (5724.8 eV) are characterized by a similar spectral signature. This group has significantly lower absorption edge energies than the second group of Ce(IV) compounds Ce(SO₄)₂ (5726.6 eV), Ce(OH)₄ (5725.4 eV), and CeO₂ (5725.5 eV). Electrons within the Ce atomic core are more tightly bound to electropositive Ce(IV) atoms, and therefore, interact with higher energy X-rays relative to Ce(III) atoms. The adsorption edge energy of the bio-Ce sample (5724.8) clearly indicates the predominance of Ce(III) precipitates. The edge energy of the samples remained constant throughout a series of three consecutive scans, and therefore, no evidence of X-ray beam induced changes was observed in any of the bacterial and model compound samples.

In addition, the samples of bio-Ce were resuspended in deionized water and the release of Ce into solution was assessed. After 24 h, no more than 5.0 ± 0.1 mg soluble Ce L⁻¹ was released from a sample containing 630 mg bio-Ce L⁻¹ (= 0.8%).

Inactivation of UZ1 by Bio-Ce. There was a clearly proportional effect of bio-Ce on the inactivation rate (Table 1); whereas no more than a 0.4 log decrease was noticed after 0.1 h when 5 mg bio-Ce L⁻¹ was added, a 1.7 and a 1.6 log decline were observed after 0.1 h upon addition of 50 and 100 mg bio-Ce L⁻¹, respectively. Moreover, addition of 250 and 500 mg bio-Ce L⁻¹ resulted in a 4 log decline after only 0.1 h (4.0 log and 4.4 log, respectively). After 2 h of contact

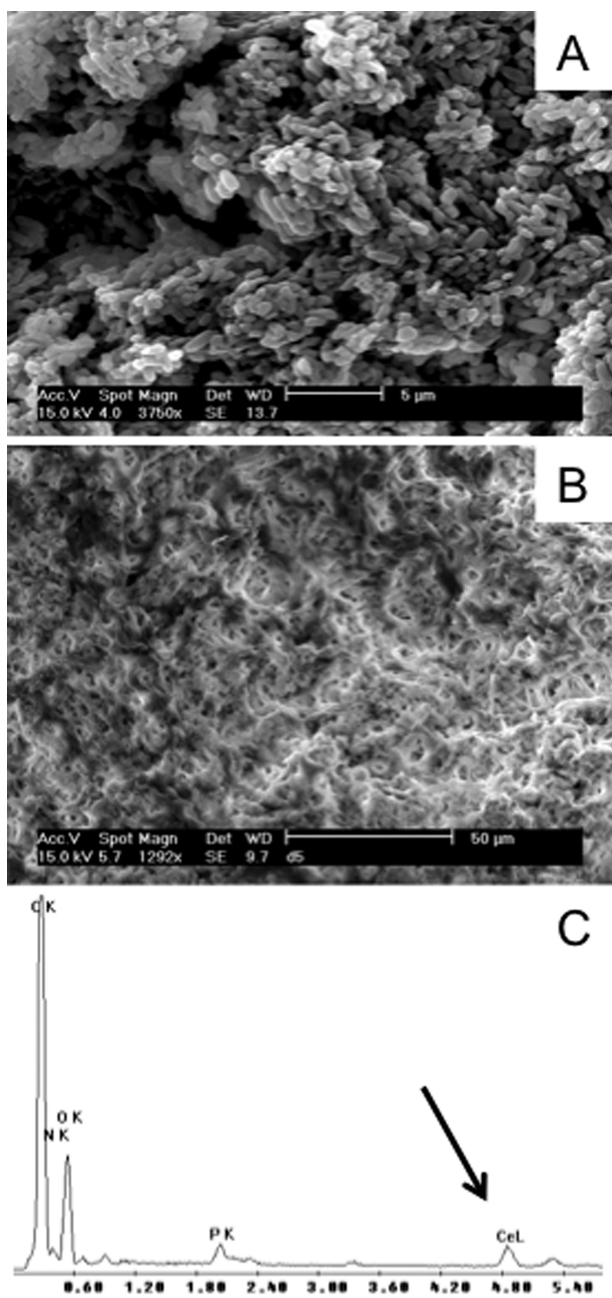


FIGURE 2. SE images of *P. putida* MnB29, grown in a medium (A) without Ce(III) (fixed) and (B) with 140 mg Ce(III) L⁻¹ (nonfixed). Figure 2C is an EDX pattern of the sample depicted in Figure 2B. The X-axis shows the energy in keV, the peaks show relative quantities of intensity (Y-axis). Part of the C peak can be related to the carbon support used for analysis.

time, there was no further removal by 5 mg bio-Ce L⁻¹. On the contrary, no phages could be detected after 2 h of contact in the case of 50, 100, 250, and 500 mg bio-Ce L⁻¹, resulting in at least a 4.4 log decrease (LOD = 100 pfu mL⁻¹).

Based on these results, further experiments were carried out using the minimal bio-Ce concentration required for a 4 log decrease in 2 h, that is, 50 mg bio-Ce L⁻¹. The results of the disinfection assays on UZ1 are depicted in Figure 4. No effect on UZ1 was observed in the biomass-free control ($C_0 = 2.7 \pm 1.7 \times 10^6$ pfu mL⁻¹). Although the addition of Ce-free biomass resulted in a modest, but significant decrease in pfu (1.2 log on average, $p = 0.001$), it was much less than that observed in the presence of 50 mg bio-Ce L⁻¹ (below LOD, ≥ 4.4 log) at 2 h ($p < 0.001$).

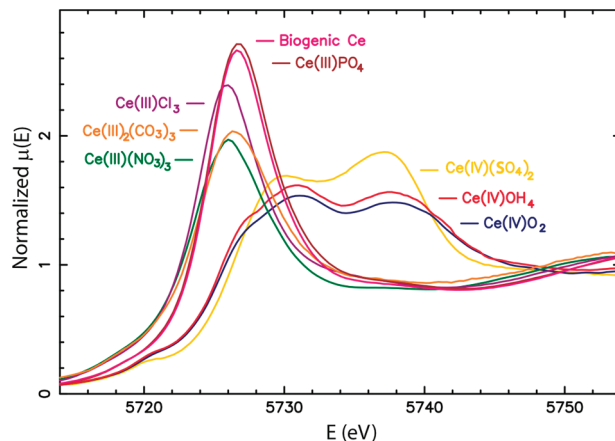


FIGURE 3. XANES spectra across the Ce L_{III} edge (ca. 5723 eV) for CeO₂, CeOH₃, Ce(SO₄)₂, CeCl₃, Ce₂(CO₃)₃·2H₂O, Ce(NO₃)₃, CePO₄·H₂O and biogenic cerium. The Bio-Ce spectral signature clearly indicates that Ce is in the +III oxidation state and the spectrum is most consistent with the CePO₄·H₂O spectrum.

TABLE 1. Inactivation of Bacteriophage UZ1 by Addition of Different Concentrations of Biogenic Cerium (Expressed as mg bio-Ce L⁻¹)^a

concentration bio-Ce (mg L ⁻¹)	$C_{0.1h}$ (pfu mL ⁻¹)	C_{2h} (pfu mL ⁻¹)
0	$2.6 \pm 0.5 \times 10^6$	$2.2 \pm 1.5 \times 10^6$
5	$1.2 \pm 2.0 \times 10^6$	$1.1 \pm 1.0 \times 10^6$
50	$5.5 \pm 4.8 \times 10^4$	<LOD
100	$7.0 \pm 5.5 \times 10^4$	<LOD
250	$2.7 \pm 1.5 \times 10^2$	<LOD
500	<LOD	<LOD

^a The concentrations of UZ1 after 0.1 and 2 h are expressed as $C_{0.1h}$ and C_{2h} , respectively. Initial phage concentration C_0 was $2.7 \pm 1.4 \times 10^6$ pfu mL⁻¹ and the LOD was 1.0×10^2 pfu mL⁻¹.

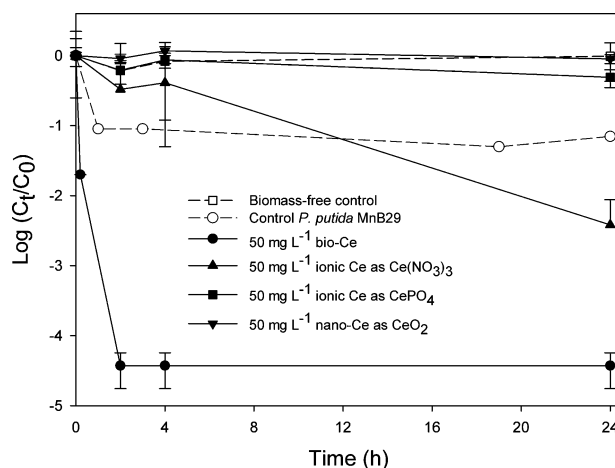


FIGURE 4. Inactivation of UZ1 in a 50 mg bio-Ce L⁻¹ suspension, compared with the biomass-free control in plain drinking water; the control with *P. putida* MnB29; the control with 50 mg L⁻¹ ionic Ce(III) (as Ce(NO₃)₃ and CePO₄·H₂O); and the control with 50 mg nano-Ce(IV) L⁻¹ (as CeO₂). C_t : concentration of bacteriophages determined by plaque assays (pfu mL⁻¹); C_0 : initial concentration. Standard deviations that not fit the logarithmic scale are not shown.

The addition of 50 mg ionic Ce(III) L⁻¹ as Ce(NO₃)₃ also resulted in a significant decline of UZ1, but at a lower rate ($p < 0.001$). After 2 h, there was a 1.2 log decrease and after 24 h, phages could still be detected above the LOD, resulting

in a 3.1 log decline (Figure 4). However, in a comparative disinfection assay with 50 mg ionic Ce(III) L⁻¹ as CePO₄·H₂O and 50 mg nano-Ce(IV) L⁻¹ as CeO₂, no significant phage removal compared to the biomass-free control was observed ($p = 0.259$ and $p = 0.397$, respectively). It should be noted that none of the Ce species exerted any observable cytotoxicity to *E. aerogenes*, which would have interfered with the plaque assays.

Discussion

Interaction of MOB with Trivalent Cerium. In this study, the interaction of MOB with Ce(III) was studied in batch incubation experiments. No more than 140 mg Ce(III) L⁻¹ was supplied since higher concentrations were reported to inhibit the growth of *Pseudomonas* sp. (2). The fact that growing bacteria were necessary for continuing sorption of Ce(III) was clearly demonstrated in the inhibition experiment with azide, a metabolic inhibitor for MOB (22). In the presence of growing MOB, a rapid decline of soluble Ce was observed, followed by a slower but continuous decrease probably due to interaction with new cells. A similar sorption pattern was observed by Sobek and Talburt (3), who studied the removal of residual supernatant Ce by *E. coli* at pH 7. These authors concluded that Ce was rapidly adsorbed by bacterial cells. Also Moffet (16) suggested this bacterial adsorption as the first and most rapid step in his two-step mechanism for Ce(III) oxidation by marine MOB.

To examine if Ce(III) oxidation took place, X-ray spectroscopy was performed to determine the predominant Ce oxidation state. Bio-Ce produced with *P. putida* was chosen for further characterization since this species was responsible for the fastest sorption of Ce(III). The results of the XPS analyses showed that Ce(III) remained in trivalent state (see Supporting Information). XANES analyses confirmed this finding and provided further indication about the nature of the bonding to the bacteria. The observed variations in the absorption edge energies and near-edge features among the different Ce(III) compounds in Figure 3 result from a complex relationship between the different bonding characteristics and local coordination environments of the Ce(III) atoms. Therefore, the essentially identical match of the bio-Ce sample spectrum with CePO₄·H₂O strongly suggests that Ce(III) was associated with phosphoryl groups on the bacterial cell surface. The quality of the spectral match indicates that impurities such as Ce-carbonates, chlorides, and nitrates or Ce(IV) compounds do not amount to more than 1–5% of the Ce in the bio-Ce samples depending on the distinguishing features of the XANES spectrum (28). Consequently, it seems unlikely that the presence of Ce(III) was the result of Ce(IV) reduction from earlier formed CeO₂ nanoparticles as suggested by Deshpande et al. (29). In addition, SEM imaging and XRD analyses did not show any crystallinity.

The accumulation of Ce(III) onto the surface of the MOB was demonstrated by Ohnuki et al. (17) as well. The authors considered the decline in Ce concentration in the medium to be the result from its adsorption by functional groups on the bacterial cell surfaces. Indeed, the outer cell membrane of Gram-negative bacteria including *Leptothrix* sp. and *Pseudomonas* sp. is known to be covered with a lipopolysaccharide layer which is negatively charged at pH 7 (30). Both carboxyl and phosphoryl groups are considered to be the main binding sites for REE (31, 32). Yet, based on the XANES spectra for both components, we suggest that Ce(III) was bound to phosphoryl groups on the bacterial carrier matrix. Thus, using modern techniques, we have provided evidence consistent with the hypothesis of Sobek and Talburt (3). Furthermore, Sobek and Talburt also suggested that there is a fixed maximal binding capacity for a given concentration of cells. Our results support this hypothesis because after the rapid sorption in the first hours of incubation, a certain

lag phase was observed before further sorption took place, especially in the case of *L. discophora*. It is likely that this phenomenon was due to rapid sorption of Ce to cells in the inoculum, followed by slow sorption to new cells after a lag in growth, which is common for *L. discophora* (A. Hay, personal communication). Yet, more research is needed to elucidate the Ce(III)-bacteria interaction and the environmental parameters influencing the mechanism of biosorption, for example by changing the functional groups on the surface of the bacterial carrier (e.g., by pH variations).

Virus Inactivation by Biogenic Cerium. In this study, bacteriophage UZ1 was used as a model for pathogenic waterborne viruses. This DNA phage can infect *E. aerogenes* BE1, a species present in normal gut microbiota (33). These phages are typically associated with human and animal excreta and indicate the potential presence of enteric viruses (34). The phage is easily and rapidly detected by plaque assay, which is a major benefit for disinfection assays (26). Moreover, somatic coliphages are in general at least as resistant to disinfectants as enteric viruses (34).

In our study, we demonstrated that bio-Ce was effective at virus removal in water. The presence of the bacterial carrier matrix significantly enhanced the removal of UZ1 by bio-Ce since, the antiviral activity exerted by Ce(III)-added as cerium nitrate at the same concentration- was lower and no virus removal was obtained by either CePO₄ or CeO₂. It is likely that adsorption to the bacterial biomass facilitated virus removal, which explains the limited 1.2 log removal of phage UZ1 in the control experiment with the same amount of biomass without cerium (Figure 4). Kim and Unno (35) have also demonstrated the reversible adsorption of viruses on activated sludge bacteria. It is generally known that the interaction of a phage with its bacterial host starts with a reversible adsorption to the cell surface (36). The affinity of phages for the bacterial cell surface likely concentrates the phages around the cells and facilitates the contact between Ce(III) and the phages for subsequent inactivation.

A minimal amount of 50 mg bio-Ce L⁻¹ was required to ensure a significant virus removal. Yet, the antiviral mechanism of Ce(III) itself still remains to be determined. Cerium nitrate has been shown experimentally to bind to the high molecular weight lipid protein complex (LPC), responsible for the immunosuppression that makes burn wounds susceptible for infections (37). Recent evidence suggests that this binding and subsequent denaturing of the LPC might be the major effect of cerium and that this is the predominant mode of action in improving survival of patients with burn wounds (6). Therefore, it might be possible that the interaction of Ce(III) with the protein capsid of the bacteriophage renders the phage noninfectious. Some authors however, have demonstrated a direct interaction between Ce(III) and DNA, and DNA damage by Ce-mediated radical production (38, 39). Additional research is needed to fully understand how bio-Ce affects the infectivity of viruses by, for example, desorption of viruses to examine the interaction with the genetic material inside the protein capsid. Furthermore, the utility of bio-Ce as an antibacterial and/or antifungal agent deserves further study but was not within the scope of this study.

The bacterial carrier clearly serves as a stabilizing agent since no more than 0.8% was released from the bio-Ce samples after 24 h. Consequently, human exposure to free Ce(III) is expected to be minimal, which is advantageous for potential future applications. Furthermore, the risk of methemoglobinemia by cerium poisoning (40) or human cell and/or tissue damage by radical production (39) is expected to be low.

Therefore, bio-Ce might have potential as a technique for disinfection of hard-to-treat waters such as those containing bromides, humic acids or chlorides since these waters cannot

be disinfected by ozonation, chlorination, UV photocatalysis, or silver based techniques (26, 41–43). Biogenic cerium represents another example of biogenic metals with practical applications for water treatment. It may be possible to encapsulate bio-Ce in polymer or silica beads or to coat it on zeolites (44) that could then be used to treat contaminated waters.

Acknowledgments

This work was supported by a PhD grant (B.D.) and project grant no. 7741-02 (T.H.) from the Research Foundation of Flanders (FWO). K.V. is a postdoctoral fellow with the FWO. This project was also funded in part by the startup package provided to D.C. by the office of the vice president for research at the University of Nevada Reno. The NSLS, J.F., and D.C. (in part) are supported by the U.S. Department of Energy, Office of Science under contract DE-AC02-98CH10886. We thank Peter Mast and Siegfried Vlaeminck for their assistance in the SEM analyses, and Diederik Depla and Nico De Roo for the XRD analyses. We are grateful for the technical assistance of Griet Vermeulen and Ellen Thibo in the disinfection assays. We acknowledge Willem De Muynck and Liesje Sintubin for critically reviewing this manuscript and Anthony Hay for the many helpful suggestions.

Supporting Information Available

Experimental details and the results of the XPS analysis. This material is available free of charge via the Internet at <http://pubs.acs.org>.

Literature Cited

- Asprey, L. B.; Cunningham, B. B. Unusual oxidation states of some actinide and lanthanide elements. In *Progress in Inorganic Chemistry*; Cotton, F. A., Ed.; John Wiley & Sons, Inc.: New York, 2007; pp 267–302.
- Burkes, S.; McCleskey, C. S. The bacteriostatic activity of cerium, lanthanum, and thallium. *J. Bacteriol.* **1947**, *54* (4), 417–424.
- Sobek, J. M.; Talburt, D. E. Effects of rare earth cerium on *Escherichia Coli*. *J. Bacteriol.* **1968**, *95* (1), 47–51.
- Jakupec, M. A.; Unfried, P.; Keppler, B. K. Pharmacological properties of cerium compounds. In *Reviews of Physiology Biochemistry and Pharmacology*; Springer-Verlag: Berlin, 2005; Vol. 153, pp 101–111.
- Monafo, W. W.; Tandon, S. N.; Ayvazian, V. H.; Tuchschildt, J.; Skinner, A. M.; Deitz, F. Cerium nitrate—New topical antiseptic for extensive burns. *Surgery* **1976**, *80* (4), 465–473.
- Garner, J. P.; Heppell, P. S. J. Cerium nitrate in the management of burns. *Burns* **2005**, *31* (5), 539–547.
- Thill, A.; Zeyons, O.; Spalla, O.; Chauvat, F.; Rose, J.; Auffan, M.; Flank, A. M. Cytotoxicity of CeO₂ nanoparticles for *Escherichia coli*. Physico-chemical insight of the cytotoxicity mechanism. *Environ. Sci. Technol.* **2006**, *40* (19), 6151–6156.
- Link, N.; Brunner, T. J.; Dreesen, I. A. J.; Stark, W. J.; Fussenegger, M. Inorganic nanoparticles for transfection of mammalian cells and removal of viruses from aqueous solutions. *Biotechnol. Bioeng.* **2007**, *98* (5), 1083–1093.
- Hennebel, T.; De Gussemme, B.; Boon, N.; Verstraete, W. Biogenic metals in advanced water treatment. *Trends Biotechnol.* **2009**, *27* (2), 90–98.
- Hennebel, T.; Simoen, H.; De Windt, W.; Verloo, M.; Boon, N.; Verstraete, W. Biocatalytic dechlorination of trichloroethylene with bio-palladium in a pilot-scale membrane reactor. *Biotechnol. Bioeng.* **2009**, *102* (4), 995–1002.
- Gadd, G. M. Microbial interactions with metals/radionuclides: the basis of bioremediation. In *Interactions of Microorganisms with Radionuclides*; Keith-Roach, M. J.; Livens, F. R., Eds.; Elsevier: New York City, 2002; pp 179–203.
- Tebo, B. M.; Bargar, J. R.; Clement, B. G.; Dick, G. J.; Murray, K. J.; Parker, D.; Verity, R.; Webb, S. M. Biogenic manganese oxides: Properties and mechanisms of formation. *Annu. Rev. Earth Planet. Sci.* **2004**, *32*, 287–328.
- Tebo, B. M.; Johnson, H. A.; McCarthy, J. K.; Templeton, A. S. Geomicrobiology of manganese(II) oxidation. *Trends Microbiol.* **2005**, *13* (9), 421–428.
- De Schampheleire, L.; Rabaey, K.; Boon, N.; Verstraete, W.; Boeckx, P. Minireview: The potential of enhanced manganese redox cycling for sediment oxidation. *Geomicrobiol. J.* **2007**, *24* (7–8), 547–558.
- Moffett, J. W. Microbially mediated cerium oxidation in seawater. *Nature* **1990**, *345* (6274), 421–423.
- Moffett, J. W. The relationship between cerium and manganese oxidation in the marine environment. *Limnol. Oceanogr.* **1994**, *39* (6), 1309–1318.
- Ohnuki, T.; Ozaki, T.; Kozai, N.; Nankawa, T.; Sakamoto, F.; Sakai, T.; Suzuki, Y.; Francis, A. J. Concurrent transformation of Ce(III) and formation of biogenic manganese oxides. *Chem. Geol.* **2008**, *253* (1–2), 23–29.
- Verthé, K.; Possemiers, S.; Boon, N.; Vaneechoutte, M.; Verstraete, W. Stability and activity of an *Enterobacter aerogenes*-specific bacteriophage under simulated gastro-intestinal conditions. *Appl. Microbiol. Biotechnol.* **2004**, *65* (4), 465–472.
- Sabirova, J. S.; Cloetens, L. F. F.; Vanhaecke, L.; Forrez, I.; Verstraete, W.; Boon, N. Manganese-oxidizing bacteria mediate the degradation of 17 α -ethinylestradiol. *Microbial Biotechnol.* **2008**, *1* (6), 507–512.
- Boogerd, F. C.; de Vrind, J. P. M. Manganese oxidation by *Leptothrix discophora*. *J. Bacteriol.* **1987**, *169* (2), 489–494.
- Greenberg, A. E.; Clesceri, L. S.; Eaton, A. D., *Standard Methods for the Examination of Waste and Wastewater*; American Public Health Society: Washington DC, 1992.
- Sunda, W. G.; Huntsman, S. A. Effect of sunlight on redox cycles of manganese in the southwestern Sargasso Sea. *Deep-Sea Res.* **1988**, *35* (8), 1297–1317.
- Mast, J.; Nanbru, C.; van den Berg, T.; Meulemans, G. Ultrastructural changes of the tracheal epithelium after vaccination of day-old chickens with the La Sota strain of Newcastle disease virus. *Vet. Pathol.* **2005**, *42* (5), 559–565.
- Cliff, G.; Lorimer, G. W. Quantitative analysis of thin specimens. *J. Microsc.-Oxf.* **1975**, *103*, 203–207.
- Ravel, B.; Newville, M. ATHENA, ARTEMIS, HEPHAESTUS: data analysis for X-ray absorption spectroscopy using IFEFFIT. *J. Synchrotron Radiat.* **2005**, *12*, 537–541.
- De Gussemme, B.; Sintubin, L.; Baert, L.; Thibo, E.; Hennebel, T.; Vermeulen, G.; Uyttendaele, M.; Verstraete, W.; Boon, N. Biogenic silver for disinfection of water contaminated with viruses. *Appl. Environ. Microbiol.* **2010**, *76* (4), 1082–1087.
- Adams, M. H., *Bacteriophages*; Interscience: New York, 1959.
- Khare, N.; Hesterberg, D.; Martin, J. D. XANES investigation of phosphate sorption in single and binary systems of iron and aluminum oxide minerals. *Environ. Sci. Technol.* **2005**, *39* (7), 2152–2160.
- Deshpande, S.; Patil, S.; Kuchibhatla, S.; Seal, S. Size dependency variation in lattice parameter and valency states in nanocrystalline cerium oxide. *Appl. Phys. Lett.* **2005**, *87* (13), 133113.
- Sonohara, R.; Muramatsu, N.; Ohshima, H.; Kondo, T. Difference in surface-properties between *Escherichia-coli* and *Staphylococcus-aureus* as revealed by electrophoretic mobility measurements. *Biophys. Chem.* **1995**, *55* (3), 273–277.
- Takahashi, Y.; Chatellier, X.; Hattori, K. H.; Kato, K.; Fortin, D. Adsorption of rare earth elements onto bacterial cell walls and its implication for REE sorption onto natural microbial mats. *Chem. Geol.* **2005**, *219* (1–4), 53–67.
- Markai, S.; Andres, Y.; Montavon, G.; Grambow, B. Study of the interaction between europium (III) and *Bacillus subtilis* fixation sites, biosorption modeling and reversibility. *J. Colloid Interface Sci.* **2003**, *262* (2), 351–361.
- Sanders, W. E.; Sanders, C. C. *Enterobacter* spp.: pathogens poised to flourish at the turn of the century. *Clin. Microbiol. Rev.* **1997**, *10* (2), 220–8.
- Grabow, W. O. K. Bacteriophages: Update on application as models for viruses in water. *Water SA* **2001**, *27* (2), 251–268.
- Kim, T. D.; Unno, H. In *The roles of microbes in the removal and inactivation of viruses in a biological wastewater treatment system*, 2nd International Symposium on Wastewater Reclamation and Reuse, Iraklion, Greece, Oct. 17–20, 1995; Pergamon-Elsevier Science Ltd: Iraklion, Greece, 1995; pp243–250.
- Weinbauer, M. G. Ecology of prokaryotic viruses. *Fems Microbiol. Rev.* **2004**, *28* (2), 127–181.
- Kremer, B.; Allgower, M.; Graf, M.; Schmidt, K. H.; Schoelmerich, J.; Schoenenberger, G. A. The present status of research in burn toxins. *Intensive Care Med.* **1981**, *7* (2), 77–87.
- Takasaki, B. K.; Chin, J. Cleavage of the phosphate diester backbone of DNA with cerium(III) and molecular-oxygen. *J. Am. Chem. Soc.* **1994**, *116* (3), 1121–1122.
- Heckert, E. G.; Seal, S.; Self, W. T. Fenton-like reaction catalyzed by the rare earth inner transition metal cerium. *Environ. Sci. Technol.* **2008**, *42* (13), 5014–5019.

- (40) Attof, R.; Magnin, C.; Bertin-Maghit, M.; Olivier, L.; Tissot, S.; Petit, P. Methemoglobinemia by cerium nitrate poisoning. *Burns* **2006**, 32 (8), 1060–1061.
- (41) Liang, L.; Singer, P. C. Factors influencing the formation and relative distribution of haloacetic acids and trihalomethanes in drinking water. *Environ. Sci. Technol.* **2003**, 37 (13), 2920–2928.
- (42) Huang, W. J.; Chang, C. Y.; Shih, F. H. Disinfection by-product formation and mutagenic assay caused by preozonation of groundwater containing bromide. *Environ. Monit. Assess.* **2009**, 158 (1–4), 181–196.
- (43) Lee, E.; Lee, H.; Jung, W.; Park, S.; Yang, D.; Lee, K. Influences of humic acids and photoreactivation on the disinfection of *Escherichia coli* by a high-power pulsed UV irradiation. *Korean J. Chem. Eng.* **2009**, 26 (5), 1301–1307.
- (44) Hennebel, T.; Verhagen, P.; Simoen, H.; De Gussemme, B.; Vlaeminck, S. E.; Boon, N.; Verstraete, W. Remediation of trichloroethylene by bio-precipitated and encapsulated palladium nanoparticles in a fixed bed reactor. *Chemosphere* **2009**, 76 (9), 1221–1225.

ES100100P